Abbreviations

%N	percentage nitrogen by mass
2-NDPA	2-Nitrodiphenylamine
ΔG	change in Gibb's free energy
ΔH	change in enthalpy
a.u.	atomic units
B3LYP	Becke, 3-parameter, Lee-Yang-Parr hybrid functional
BCP	bonding critical point
CH_3CH_3	NC repeat unit with two methoxy capping groups
CH_3OH	NC repeat unit with methoxy capping group on ring 1, hydroxy group on ring 2
CCP	cage critical point
CP	critical point
DFT	density functional theory
DOS	degree of substitution
DPA	diphenylamine
EM	energetic materials
ESP	electrostatic potential
G09	Gaussian 09 revision D.01

GM	genetically modified
GView	Gauss View 5.0.8
HF	Hartree Fock theory
IR	infra-red spectroscopy
MEP	minimum energy path
MM	molecular mechanics
MMFF94	Merck molecular force field 94
MW	molecular weight
NC	nitrocellulose
NCP	nuclear critical point
NG	nitroglycerine
NMR	nuclear magnetic resonance spectroscopy
OHCH$_3$	NC repeat unit with hydroxy capping group on ring 1, methoxy group on ring 2
PCM	polarisable continuum model
PES	potential energy surface
PETN	pentaerythritol tetranitrate
QM	quantum mechanics
QTAIM	quantum theory of atoms in molecules
RCP	ring critical point
SB59	1,4-bis(ethylamino)-9,10-anthraquinone dye
SEM	scanning electron microscopy
S$_N$2	bi-molecular nucleophilic substitution reaction

TS   transition state

UFF   universal force field

UV   ultraviolet

UV-Vis   ultraviolet–visible spectroscopy

ωB97X-D ωB97X-D long-range corrected hybrid functional

Chapter 2

Nitration and Denitration Sequence of Nitrocellulose

[Added as preamble for Chapter 4 below]

[Review usage of NO$_x$ for consistency with the whole text. Maybe just stick to "nitrous oxides" for the whole document.]

2.1 Introduction

Moniruzzaman *et al.* used the UV absorption of an anthraquinone dye to determine the activation energies for the removal of the nitrate at C2, C3, C6 sites on nitrocellulose (NC) (figure 2.1)[1, 2]. UV-Vis was chosen as an efficient, non-destructive method of monitoring the decomposition process. The reaction of the 1,4-bis(ethylamino)-9,10-anthraquinone dye (SB59) with NO$_x$ released by denitration, mimics the action of stabilisers such as diphenylamine (DPA) and 2-Nitrodiphenylamine (2-NDPA) commonly used in NC formulations. The secondary amine groups of the dye consume any nitrates in the system, eliminating the possibility of successive reactions generating acidic species. The presence of acid has been linked to autocatalytic rates of degradation during later stages of NC degradation[3, 4, 5, 6].

Un-aged NC thin films and films aged at 40°C, 50°C, 60°C and 70°C for timescales of up to 2000hrs for 40°C, were compared. Decreasing absorption peak intensity of the dye and appearance of new absorption regions gave insight into the extent of denitration and the presence of secondary reaction products (figure 2.2). The NC starting material was 12.15%N by mass, with mean degree of substitution (DOS)=2.307, indicating that individual glucopyranose rings were of mixed nitration level with non-uniform distribution of nitrate groups along the polymer. The study found that the nitrate at the C3 position would
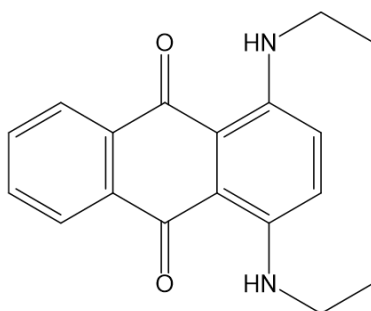
Figure 2.1: 1,4-bis(ethylamino)-9,10-anthraquinone dye (SB59) used to probe the release of nitrates from NC using ultraviolet–visible spectroscopy (UV-Vis) and ^{1}H NMR spectroscopy[2].
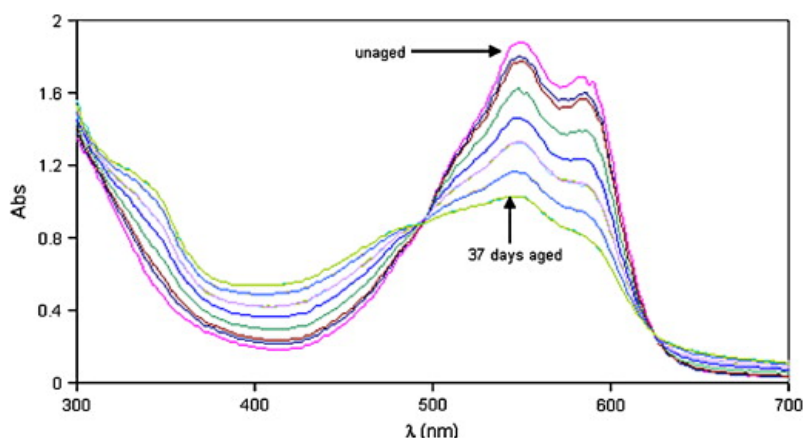
Figure 2.2: UV spectra of NC thin films with and without accelerated ageing at 60 °C, over a total time of 37 days, from the work of Moniruzzaman *et al.*[1]. The unaged peak demonstrates a strong absorbance in the region corresponding to the SB59 dye (. This decreases as the dye is consumed in the reaction of NO$_x$ released upon NC denitration.

be most reactive, possessing the lowest activation barrier to removal. This was followed by C2 and C6. The findings contrast with the computational work of Shukla *et al.*, who determined that denitration via alkyaline hydrolysis followed the order of C3→C6→C2 [7, 8]. In this case, the study only considered the fully nitrated system. There is evidence that nitration and denitration are influenced by the presence of nitrate groups at adjacent positions. Matveev *et al.* demonstrated that for polynitro esters the rate of liquid-phase decomposition did not increase linearly with number of nitrate reaction centres, but was mainly dependent on individual structures table 4.1[9]. It was suggested that the trend in reactivity could be explained by the inductive effect of nitrate groups.

The inductive effect arises when a difference in the electronegativity between atoms connected by a σ bond leads to a polarisation, or permanent dipole, in the bond. Electron donating groups increase the δ- partial charge on neighbouring atoms through the release of electrons, whilst electron withdrawing groups pull electron density away from neighbouring

Table 2.1: Comparison of rate constants of decomposition for various polynitrate esters at 140°C. Collated from literature sources by Matveev *et al.*[9].

Compound	ΔT / °C	E / kcal mol^{-1}	$\log A$ [s^{-1}]	k_{expt} / 10^{-6} s^{-1}
$O_2NOCH_2CH_2CH_2ONO_2$	72–140	39.1	14.9	1.7
$O_2NOCH_2CH_2CH_2CH_2ONO_2$	100–140	39.0	14.7	1.1
$O_2NOCH(CH_3)CH(CH_3)ONO_2$	72–140	40.3	14.9	5.0
$O_2NOCH_2CH_2OCH_2CH_2ONO_2$	80–140	42.0	16.5	1.9
$O_2NOCH_2CH(OH)(CH_2ONO_2)$	80–140	42.4	16.8	2.3
$O_2NOCH_2CH(ONO_2)(CH_3)$	72–140	40.3	15.8	3.0
$[(O_2NOCH_2)CH(ONO_2)CH(ONO_2)]_2$ (hexanitromannite)	80–140	38.0	15.9	63.0

atoms generating a $\delta+$ charge on connected atoms. From the studies above, it is seen that the denitration order of NC can be influenced by the location, distribution and saturation of the nitrated sites along the polymer, as well as mechanistic differences in thermal and chemical degradation. Crucially, a synergistic effect leading to facile removal of the C3 group when the C2 site is also nitrated may play an important part in the decomposition pathway. The DOS value of the source NC would therefore give an indication of the likelihood of adjacent nitrates.

Chapter 4

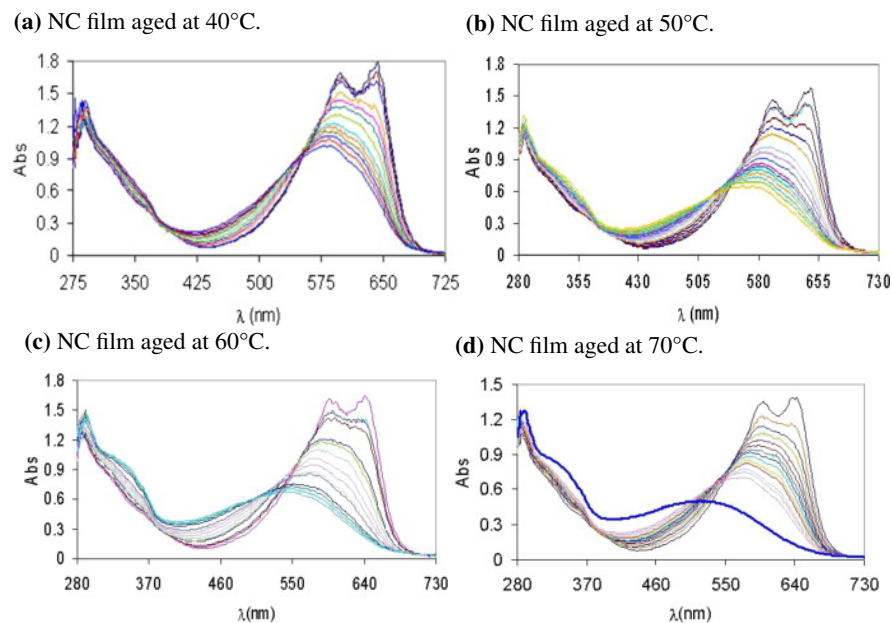# Post-Denitration Reactions

4.1   Introduction

Products of the preliminary denitration step of NC can be evolved as gases or remain trapped in the polymer matrix. Reactive nitrous oxide radicals generated from homolysis of the O-N bond are likely to migrate within the bulk and attack other sites on the polysaccharide. Nitrous and nitric acids released directly from denitration, or via transformation of released NO_x species, contribute to the acidity of the overall system, lowering the pH and stimulating further hydrolysis processes.

When studying the ageing of NC using UV-Vis spectroscopy, Moniruzzaman *et al.* observed increasing concentrations of secondary reaction products following heat treatment over extended timescales* (figure 4.1) [1, 2]. UV absorbances at 600 nm and 650 nm were characteristic of the SB59 dye used to indicate the presence of NO_x, released by the denitration of NC. The isosbestic point identified at 552 nm showed that as the concentration of SB59 decreased, the concentration of the [SB59 + NC] product increased. For measurements >40°C, the isosbestic point demostrated a shift downwards. This was most clearly illustrated by the 70°C case, whereby the final measurement (indicated by the royal-blue line in bold) deviated from the isosbestic point entriely, and presented more than 81% consumption of the original dye concentration. The drift of the isosbestic point with the appearance of new peaks below 400 nm suggests the presence of additional species in the reaction mixture. It is likely that these arise from the continued reaction of SB59 derivatives with NC degradation products, or further derivatives thereof, as suggested in scheme 4.1.

Following the possible denitration routes outlined in Chapter 3, the remaining residues are available for further reaction with the polymer or other free molecules in the system.

---

*First introduced in section 2.1

(a) NC film aged at 40°C.

(b) NC film aged at 50°C.

(c) NC film aged at 60°C.

(d) NC film aged at 70°C.

Figure 4.1: UV-Vis spectra of aged NC-based film, from the work of Moniruzzaman *et al.*[2]. The peaks at 600 nm and 650 nm are attributed to the π - π^* transitions in the anthraquinone dye (SB59). Spectral lines with highest absorbance in this region correspond to the sample prior to heat treatment. Peaks below 400 nm indicate the formation of SB59 derivatives due to secondary reactions.
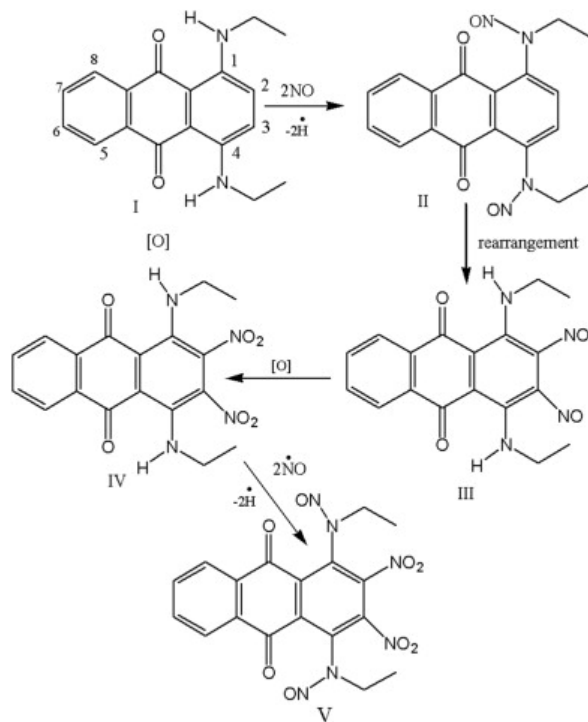
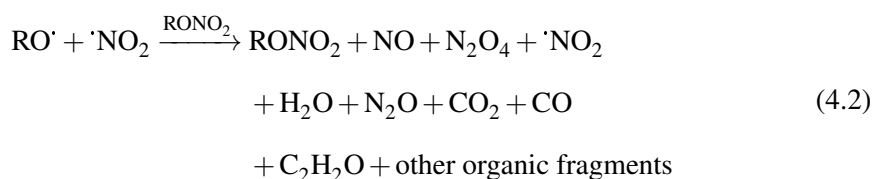**Scheme 4.1:** Proposed reaction pathway for the the SB59 dye with NOx released as a result of denitration of NC [2].

Chin *et al.* proposed schemes for the propagation of such reactions initated by both thermolysis and hydrolysis of nitrate esters [**?**] :
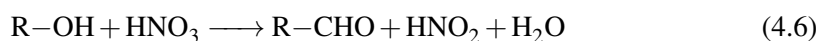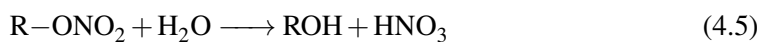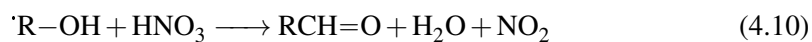
Thermolysis

Initiation:

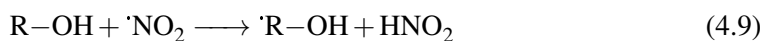$$RONO_2 \longrightarrow RO^{\cdot} + {}^{\cdot}NO_2 \tag{4.1}$$

Propagation:

$$RO^{\cdot} + {}^{\cdot}NO_2 \xrightarrow{RONO_2} RONO_2 + NO + N_2O_4 + {}^{\cdot}NO_2$$
$$+ H_2O + N_2O + CO_2 + CO \tag{4.2}$$
$$+ C_2H_2O + \text{other organic fragments}$$

$$2\,{}^{\cdot}NO + O_2 \longrightarrow 2\,{}^{\cdot}NO_2 \tag{4.3}$$

$$2\,{}^{\cdot}NO_2 \longleftrightarrow N_2O_4 \tag{4.4}$$

Hydrolysis

Initiation:

$$R{-}ONO_2 + H_2O \longrightarrow ROH + HNO_3 \tag{4.5}$$

$$R{-}OH + HNO_3 \longrightarrow R{-}CHO + HNO_2 + H_2O \tag{4.6}$$

Propagation:

$$HNO_3 + HNO_2 \longrightarrow N_2O_4 + H_2O \tag{4.7}$$

$$N_2O_4 \longrightarrow 2\,{}^{\cdot}NO_2 \tag{4.8}$$

$$R{-}OH + {}^{\cdot}NO_2 \longrightarrow {}^{\cdot}R{-}OH + HNO_2 \tag{4.9}$$

$${}^{\cdot}R{-}OH + HNO_3 \longrightarrow RCH{=}O + H_2O + NO_2 \tag{4.10}$$
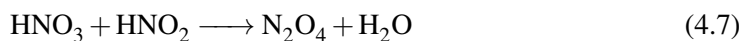
The hydrolysis equations were modified from an earlier work by Camera *et al.*, where the scheme was presented with ethyl nitrate as the organonitrate (where $R = CH_3CH_2$) [**?**]. The rate-determining nature of equation 4.6
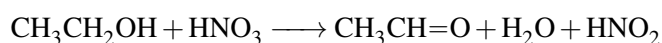
It is widely agreed that first-stage decomposition follows a first-order process (or pseudo-first order, with respect to hydrolysis reactions). A number of studies observe cat-

alytic rate of decay for the longer-term aging processes. Dauerman [10] observed that when NC was treated with NO_2 gas before heating, the time required for sample ignition halved. He suggested that the NO_2 adsorbed onto the surface acted as a catalysing agent.
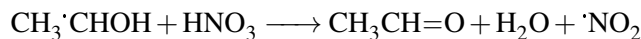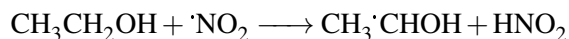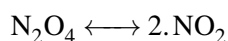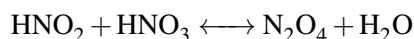
Neutral and alkaline hydrolysis reactions follow a pseudo-first order process, however it has been suggested that the presence of acid faciltiatles a catalyic rate of degradation after an initial incubation period.

Multiple studies have addressed the decomposition reactions of nitrate esters following the initial scission of the nitrate group [**?**, 5, **?**, **?**, 9, **?**]
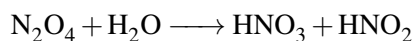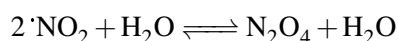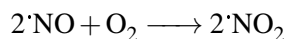
Initiation

$$CH_3CH_2OH + HNO_3 \longrightarrow CH_3CH{=}O + H_2O + HNO_2$$

Propagation

$$HNO_2 + HNO_3 \longleftrightarrow N_2O_4 + H_2O$$
$$N_2O_4 \longleftrightarrow 2.NO_2$$
$$CH_3CH_2OH + {}^{\cdot}NO_2 \longrightarrow CH_3{}^{\cdot}CHOH + HNO_2$$
$$CH_3{}^{\cdot}CHOH + HNO_3 \longrightarrow CH_3CH{=}O + H_2O + {}^{\cdot}NO_2$$

Aellig's equations

Initiation

$$4\,HNO_3 \rightleftharpoons 4\,NO_2 + 2\,H_2O + O_2$$
$$2\,{}^{\cdot}NO_2 + H_2O \rightleftharpoons N_2O_4 + H_2O$$
$$N_2O_4 + H_2O \longrightarrow HNO_3 + HNO_2$$

Propagation

$$CH_3CH_2OH + HNO_2 \longleftrightarrow CH_3CH_2ONO + H_2O$$
$$CH_3CH_2ONO \longrightarrow CH_3CH{=}O + HNO$$
$${}^{\cdot}NO_2 + HNO \longrightarrow HNO_2 + {}^{\cdot}NO$$
$$2\,{}^{\cdot}NO + O_2 \longrightarrow 2\,{}^{\cdot}NO_2$$

Termination

$$HNO + HNO \longrightarrow HON{=}NOH$$

$$HON{=}NOH \longrightarrow N_2O + H_2O$$
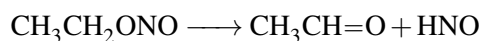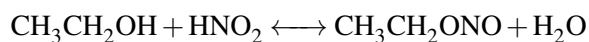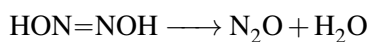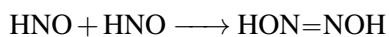
In this section, secondary and extended reaction schemes for the low temperature ageing of NC are explored. Decompostition pathways defined by Camera *et al.* and Aellig *et al.* are probed to determine the reactions responsible for the experimentally observed degradation products. The reactions found to be energetically feasible from the proposed routes will be scrutinised to determine whether an autocatalytic pathway can be formed from the energitcally validated reaction schemes.

4.2 Methodology

The species reactions proposed by Camera and Aellig *et al.* were geometry optimised using ωB97X-D long-range corrected hybrid functional (ωB97X-D), and Becke, 3-parameter, Lee-Yang-Parr hybrid functional (B3LYP) functionals, in both vacuum and solvent. The reactions were modelled using ethyl nitrate as a test system before expansion to the full C2 monomeric model. The change in Gibb's free energy (ΔG) were used to determine the feasibility of a reaction. Where the choice of method lead to a variation in the result

4.2.1 Computational details

All geometry optimisations were performed in Gaussian 09 revision D.01 (G09), using the ωB97X-D and B3LYP functionals. Optimisations were repeated with polarisable continuum model (PCM) to introduce solvent effects.

4.3 Results and Discussion

4.3.1 Thermodynamics of Ethyl Nitrate reactions

Table 4.1: Free energies of protonation at different oxygens sites on ethyl nitrate.

Protonation site	ΔG_r		ΔH_r	
	ωB97X-D	PCM	B3LYP	PCM
Terminal (up) O $CH_3CH_3ONO_2H^+$	0.0072	0.0083	0.0064	0.0077
Terminal (down) O	-0.0195	0.0140	-0.0219	0.0101
Bridging O	-0.0195	0.0140	-0.0219	0.0101

4.3.1.1 Radical mechanistic route

4.3.1.2 Ionic mechanistic route

4.3.2 Reactions of Nitrocellulose Monomer

4.4 Summary

Bibliography

[1] M. Moniruzzaman and J.M. Bellerby. Use of UV–visible spectroscopy to monitor nitrocellulose degradation in thin films. *Polymer Degradation and Stability*, 93(6):1067–1072, jun 2008.

[2] Mohammed Moniruzzaman, John M. Bellerby, and Manfred A. Bohn. Activation energies for the decomposition of nitrate ester groups at the anhydroglucopyranose ring positions C2, C3 and C6 of nitrocellulose using the nitration of a dye as probe. *Polymer Degradation and Stability*, 102:49–58, apr 2014.

[3] M. Edge, N.S. Allen, M. Hayes, P.N.K. Riley, C.V. Horie, and J. Luc-Gardette. Mechanisms of deterioration in cellulose nitrate base archival cinematograph film. *European Polymer Journal*, 26(6):623–630, jan 1990.

[4] Mª Ángeles Fernández de la Ossa, María López-López, Mercedes Torre, and Carmen García-Ruiz. Analytical techniques in the study of highly-nitrated nitrocellulose. *TrAC Trends in Analytical Chemistry*, 30(11):1740–1755, dec 2011.

[5] John W. Baker and D. M. Easty. Hydrolytic decomposition of esters of nitric acid. Part I. General experimental techniques. Alkaline hydrolysis and neutral solvolysis of methyl, ethyl, isopropyl, and tert.-butyl nitrates in aqueous alcohol. *Journal of the Chemical Society (Resumed)*, 1952(0):1193–1207, 1952.

[6] N. Binke, L. Rong, Y. Zhengquan, W. Yuan, Y. Pu, Hu Rongzu, and Y. Qingsen. Studies on the Kinetics of the First Order Autocatalytic Decomposition Reaction of Highly Nitrated Nitrocellulose. *Journal of Thermal Analysis and Calorimetry*, 58(2):403–411, 1999.

[7] Manoj K. Shukla and Frances Hill. Theoretical investigation of reaction mechanisms of alkaline hydrolysis of 2,3,6-trinitro-β-d-glucopyranose as a monomer of nitrocellulose. *Structural Chemistry*, 23(6):1905–1920, apr 2012.

[8] Manoj K Shukla and Frances Hill. Computational elucidation of mechanisms of alkaline hydrolysis of nitrocellulose: dimer and trimer models with comparison to the corresponding monomer. *The journal of physical chemistry. A*, 116(29):7746–55, 2012.

[9] V. G. Matveev and G. M. Nazin. Stepwise Degradation of Polyfunctional Compounds. *Kinetics and Catalysis*, 44(6):735–739, nov 2003.

[10] L. Dauerman and Y. A. Tajima. Thermal decomposition and combustion of nitrocellulose. *AIAA Journal*, 6(8):1468–1473, aug 1968.